Int. J. Heat Mass Transfer. Vol. 29, No. 4, pp. 563–572, 1986
Printed in Great Britain

0017–9310/86 $3.00 + 0.00
© 1986 Pergamon Press Ltd.

A numerical study of thermocapillary flow in a rectangular cavity during laser melting

J. SRINIVASAN* and BISWAJIT BASU†

* Mechanical Engineering Department, Indian Institute of Science, Bangalore 560 012, India
† Tata Research Development and Design Centre, Pune 411 001, India

(*Received* 21 *May* 1985)

Abstract—The surface tension gradient driven flow that occurs during laser melting has been studied. The vorticity–streamfunction form of the Navier–Stokes equations and the energy equation has been solved by the 'Alternative Direction Implicit' method. It has been shown that the inertia forces in the melt strongly influence the flow pattern in the melt. The convection in the melt modifies the isotherms in the melt at high surface tension Reynolds number and high Prandtl number. The buoyancy driven flow has been shown to be negligible compared to the surface tension gradient driven flow in laser melting.

INTRODUCTION

LASER surface melting and alloying can be used to produce a surface layer with desired properties such as wear and corrosion resistance. When a laser beam impinges on a surface there can be a large difference in the temperature of the surface beneath the centre of the laser beam and that beneath the edge of the laser beam. This temperature difference along the free surface of the molten material causes variation in surface tension along the free surface. The variation in surface tension along the free surface causes fluid motion which is called 'thermocapillary flow'. Fluid flow during laser melting can influence the composition and structure of the solidified material. The knowledge of temperature and velocity profile in the melt is essential to predict the scale and character of the microstructure.

Mehrabian *et al.* [1] have reported the relationship between microstructure and fluid flow pattern when an aluminium–copper alloy was subject to laser melting and solidification. A continuous carbon dioxide laser with a power density of 10^6 W cm^{-2} was used. A study of the microstructure by Mehrabian *et al.* [1] revealed a circular convection pattern just below the melt. Structural analysis revealed that vigorous convection occurred in the middle of the melt.

Anthony and Cline [2] have obtained an analytical solution of the Navier–Stokes equations in order to predict the fluid flow induced by surface tension gradients during laser melting. Their analysis assumed that the inertia forces are negligible in the melt. The results obtained by them indicate, however, that the Reynolds number for the flow can be as high as 10,000. Hence the neglect of inertia forces by Anthony and Cline [2] cannot be justified. If both inertia and viscous forces are included in the Navier–Stokes equations it is not possible to obtain simple analytical solutions. Hence the fluid flow and temperature profiles in the melt must be obtained by numerical solution of the Navier–Stokes equations and the energy equation.

In this paper we study the flow pattern and temperature variation in a surface tension driven flow in a molten cavity. The molten region is assumed to be a long, rectangular cavity with the side and bottom walls at the melting temperature of the material. The top free surface of the material is assumed to have a sinusoidal variation of temperature with the maximum temperature at the centre and minimum surface temperature at the edge (see Fig. 1). The temperature and velocity profiles in the melt are obtained by the solution of the Navier–Stokes equations and the energy equation by a finite-difference method.

BASIC EQUATIONS

The flow induced by the surface tension gradient is governed by the Navier–Stokes equations. In the present problem it is convenient to write these in the vorticity–streamfunction form rather than the primitive form. The Navier–Stokes equations in the primitive variables demand the specification of boundary conditions on pressure. This is difficult to specify in this problem and hence, for cavity flows, the vorticity–streamfunction form of these equations is generally preferred. The Navier–Stokes equations in the vor-

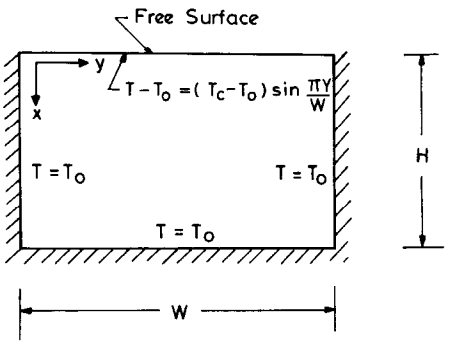

FIG. 1. Coordinate system.

NOMENCLATURE

A	aspect ratio	μ	dynamic viscosity [kg m^{-1} s^{-1}]
g	acceleration due to gravity [m s^{-2}]	ν	kinematic viscosity [m^2 s^{-1}]
Gr	Grashof number	σ	surface tension [N m^{-1}]
H	height of the cavity [m]	Ψ	streamfunction [m^2 s^{-1}]
Ma	Marangoni number	ω	vorticity [s^{-1}].
R_σ	surface tension Reynolds number		
t	time [s]		
T	temperature [K]	Subscripts	
U	vertical velocity [m s^{-1}]	c	centre of the cavity
V	horizontal velocity [m s^{-1}]	0	edge of the cavity
W	width of the cavity [m]	r	reference.
X	vertical coordinate [m]		
Y	horizontal coordinate [m].		
Greek symbols		Superscript	
α	thermal diffusivity [m^2 s^{-1}]	*	nondimensional variable.
β	coefficient of volumetric expansion [K^{-1}]		

ticity–streamfunction form are (see, for example [3])

$$\frac{\partial\omega}{\partial t}+U\frac{\partial\omega}{\partial X}+V\frac{\partial\omega}{\partial Y}=g\beta\frac{\partial T}{\partial Y}+\nu\left[\frac{\partial^2\omega}{\partial X^2}+\frac{\partial^2\omega}{\partial Y^2}\right] \quad (1)$$

$$\omega=-\left(\frac{\partial^2\psi}{\partial X^2}+\frac{\partial^2\psi}{\partial Y^2}\right) \quad (2)$$

where

$$\omega=\frac{\partial V}{\partial X}-\frac{\partial U}{\partial Y}$$

$$U=\frac{\partial\psi}{\partial Y}$$

$$V=-\frac{\partial\psi}{\partial X}.$$

The energy equation can be written as

$$\frac{\partial T}{\partial t}+U\frac{\partial T}{\partial X}+V\frac{\partial T}{\partial Y}=\alpha\left(\frac{\partial^2 T}{\partial X^2}+\frac{\partial^2 T}{\partial Y^2}\right). \quad (3)$$

The initial conditions are

$$t=0,\quad U=V=\omega=0,\quad T=T_0$$
$$\left.\begin{array}{l}0<X<H\\0<Y<W\end{array}\right\}. \quad (4)$$

The boundary conditions are ($t>0$)

$$U=V=\psi=0,\quad T=T_0$$

for

$$\left.\begin{array}{ll}Y=0,W & 0<X<H\\X=H & 0<Y<W\end{array}\right\} \quad (5)$$

$$U=0,\quad \psi=0,\quad T=T_0+(T_c-T_0)\sin(\pi Y/W) \quad (6)$$

for $X=0,\ 0<Y<W$

$$\omega=\frac{\partial V}{\partial X}=-\frac{1}{\mu}\left(\frac{d\sigma}{dT}\right)\frac{\partial T}{\partial Y} \quad (7)$$

for $X=0,\ 0<Y<W$.

The boundary condition at the surface [equation (7)] represents the balance between shear stress and surface tension gradient at the surface. This boundary condition is responsible for the establishment of thermocapillary flow in the cavity. The above equations and boundary conditions incorporate the following assumptions.

1. The flow is laminar.
2. The fluid is incompressible.
3. The free surface of the fluid is flat.
4. The Boussinesq approximation is valid for density variation.

In the case of thermocapillary flows the conditions under which the onset of turbulence occurs is not well understood. Hence the assumption that the thermocapillary flow in the cavity is laminar is, at best, a first approximation, in the absence of adequate data on the onset of turbulence. It is reasonable to assume that the fluid is incompressible since the velocities encountered in this type of flow are expected to be much lower than the sonic velocity in the fluid. The free surface of the fluid has been assumed to be flat and this may seem to be a drastic assumption. Sen and Davis [4], who considered the asymptotic solutions for thermocapillary flow in a cavity, have shown that this assumption is justified if the capillary number is much less than 1. The capillary number is defined as $\Delta\sigma/\bar{\sigma}$ where $\Delta\sigma$ is the maximum difference in surface tension and $\bar{\sigma}$ is the mean value of surface tension. The capillary number is

much less than 1 for most molten metals during laser melting.

The numerical solution of the Navier–Stokes equations and energy equation will be easier if we non-dimensionalise the independent and dependent variables. This will enable us to identify the non-dimensional parameters relevant to this problem. We choose the non-dimensional variables as

$$X^* = X/H, \quad Y^* = Y/W, \quad T^* = (T-T_0)/(T_c-T_0),$$
$$A = H/W, \quad U^* = U/U_r A, \quad V^* = V/U_r,$$
$$t^* = tU_r/W, \quad \psi^* = \psi/U_r W \quad \text{and} \quad \omega^* = \omega W/U_r.$$

The manner in which the variables X, Y and T have been made non-dimensional should need no explanation. The choice of reference velocity U_r for non-dimensionalising U, V, t, ω and ψ needs careful thought. We do not have, at this stage, any idea of the magnitude of the velocities in the melt. We know, however, that the flow is driven primarily by the shear stress induced at the surface by the surface tension gradient. The shear stress boundary condition, at the surface, can be used to obtain an estimate of the order of magnitude of the velocity in the melt. Let us assume that the characteristic velocity in the melt is U_r and use this to non-dimensionalise the velocity in the shear stress boundary condition at the interface

$$\frac{\partial V^*}{\partial X^*} = -\frac{1}{U_r}\left(\frac{d\sigma}{dT}\right)\frac{(T_c-T_0)H}{W}\frac{\partial T^*}{\partial Y^*};$$
$$X^* = 0, \quad 0 < Y^* < 1.$$

If we assume that $U_r = -(d\sigma/dT)[(T_c-T_0)H/\mu W]$, the non-dimensional boundary condition at the interface becomes

$$\frac{\partial V^*}{\partial X^*} = \frac{\partial T^*}{\partial Y^*}; \quad X^* = 0, \quad 0 < Y^* < 1.$$

The above form of the boundary condition implies that shear stress and surface tension gradient are in balance at the interface. If we had not assumed U_r to be in the above form, a parameter would have appeared in the shear stress boundary condition. If this parameter had very small or very large values it would make one term in the above boundary condition much larger than the other. This would have made the shear stress boundary condition at the interface take a trivial form. Since thermocapillary flow is driven by the shear stress at the surface we cannot let this boundary condition take a trivial form.

The non-dimensional form of the Navier–Stokes equations and energy equation can now be written as

$$\frac{\partial \omega^*}{\partial t^*} + U^*\frac{\partial \omega^*}{\partial X^*} + V^*\frac{\partial \omega^*}{\partial Y^*} = \frac{Gr}{R_\sigma^2}\frac{\partial T^*}{\partial Y^*} + \frac{1}{R_\sigma}\left[\frac{\partial^2 \omega}{\partial Y^{*2}} + \frac{1}{A^2}\frac{\partial^2 \omega}{\partial X^{*2}}\right] \quad (8)$$

$$\omega^* = -\left(\frac{1}{A^2}\frac{\partial^2 \psi^*}{\partial X^{*2}} + \frac{\partial^2 \psi^*}{\partial Y^{*2}}\right) \quad (9)$$

$$\frac{\partial T^*}{\partial t} + U^*\frac{\partial T^*}{\partial X^*} + V^*\frac{\partial T^*}{\partial Y^*} = \frac{1}{R_\sigma Pr}\left[\frac{\partial^2 T^*}{\partial Y^{*2}} + \frac{1}{A^2}\frac{\partial^2 T^*}{\partial X^{*2}}\right]. \quad (10)$$

Initial conditions

$$t^* = 0, \quad T^* = U^* = V^* = \omega^* = \psi^* = 0 \quad \left.\begin{matrix} 0 < X^* < 1 \\ 0 < Y^* < 1 \end{matrix}\right\}. \quad (11)$$

Boundary conditions ($t^* \geqslant 0$)

$$U^* = V^* = \psi^* = T^* = 0; \quad \left.\begin{matrix} Y^* = 0,1 & 0 < X^* < 1 \\ X^* = 1 & 0 < Y^* < 1 \end{matrix}\right\} \quad (12)$$

$$\left.\begin{matrix} U^* = V^* = 0 \\ T^* = \sin \pi Y^* \end{matrix}\right\} X^* = 0, \quad 0 < Y^* < 1 \quad (13)$$

$$\omega^* = \partial T^*/\partial Y^*; \quad X^* = 0, \quad 0 < Y^* < 1. \quad (14)$$

From the above equations we see that there are four non-dimensional parameters in the study of thermocapillary flow in a cavity. They are:

1. Aspect ratio, $A = H/W$.
2. Surface tension Reynolds number $R_\sigma = U_r W/\nu$.
3. Grashof number, $Gr = g\beta(T_c-T_0)W^3/\nu^2$.
4. Prandtl number $Pr = \nu/\alpha$.

The product $R_\sigma\, Pr$ is also known as the Marangoni number. The ratio Gr/R_σ^2 determines the importance of the buoyancy driven flow as compared to the surface tension driven flow in the cavity. For a typical laser melting problem $W = L = 0.001$ m and $T_c - T_0 = 200$ K. For molten iron, $d\sigma/dT = -0.0004$ N m^{-1} K^{-1}, $\beta = 0.001$ K^{-1}, $\mu = 0.008$ kg m^{-1} s^{-1}, $\nu = 10^{-6}$ m^2 s^{-1}, $\alpha = 10^{-5}$ m^2 s^{-1}. Hence for laser melting of iron, $R_\sigma = 10{,}000$ while $Gr = 1960$. Therefore Gr/R_σ^2 is equal to 1.96×10^{-5}. We can, therefore, neglect the buoyancy driven flow as compared to the surface tension driven flow in laser melting.

NUMERICAL SCHEME

The standard finite-difference technique for the numerical solution of the vorticity equation and the energy equation is the Alternative Direction Implicit (ADI) scheme. The central-difference scheme was used for all space derivatives. The use of the central-difference scheme for the convective terms in the vorticity and energy equation resulted in very slow convergence of the vorticity equation (or the energy equation) for surface tension Reynolds number (or Marangoni number) above 1750. Hence we used the upwind-difference scheme for the convective terms in the vorticity equation and the energy equation. We used the second upwind-difference scheme which has been shown to be superior to the first upwind-difference scheme by Torrance [5]. For the solution of the

vorticity equation the values of the vorticity at the wall are required. The wall vorticities are obtained by expanding the streamfunction in a Taylor series. We can then obtain the wall vorticities as follows (see Roache [6] for further details)

$$\omega_w^* = -\frac{2\psi_{w+1}^* A^2}{(\Delta w)^2} \tag{15}$$

where the subscripts w and $w+1$ denote the grid points at the wall and close to the wall respectively, and Δw denotes grid spacing. The equation relating streamfunction to vorticity [equation (9)] was solved by the successive over-relaxation method. The optimum value of the relaxation parameter was 1.58. If the primary aim is to study the steady-state solution, rapid convergence to steady state can be obtained by employing an interior loop while solving the vorticity equation [equation (8)] and streamfunction equation [equation (9)]. The solution of the finite-difference form of the vorticity equation gives the value of vorticity at interior points for the specified value of wall vorticity [from equation (15)]. The new values of vorticity at interior points can now be used to find the new value of the streamfunction by solving the finite-difference form of the streamfunction equation [equation (9)]. The new value of streamfunctions at the interior points enable us to obtain the new value of wall vorticities through equation (15). The vorticity equation is now solved with the new value of wall vorticity. The entire cycle is repeated many times till the streamfunction remains unchanged to within 0.1%. This approach is discussed in more detail by Szekely and Todd [7]. The finite-difference form of the energy equation is now solved using the accurate value of streamfunction obtained from the previous step. The most commonly used method for ascertaining whether steady state has been reached is the relative error criterion.

$$\max_{i,j} \left| \frac{P_{ij}^{n+1} - P_{ij}^n}{P_{ij}^n} \right| < \varepsilon, \quad P_{ij}^n \neq 0$$

where P_{ij}^n is any variable, such as velocity, vorticity, or temperature at the grid point i, j and time level n. This method of ascertaining the steady state can give misleading results if the time step chosen for marching is very small. A more reliable method is to compare the transient term in the vorticity (or energy) equation with other terms in that equation. When the transient term is less than 1% of the most significant term in that equation we can confidently claim that steady state has been reached.

The use of an upwind-differencing scheme for convective terms contributes to artificial viscosity. The contribution made by artificial viscosity can be reduced by using a smaller grid size. We found that a 41×41 grid was essential to reduce the contribution of artificial viscosity and obtain an accurate solution. For surface tension Reynolds number in the range 100–15,000 (and 41×41 grid) we found that the time step that can be chosen without encountering instability was

$$\Delta t^* < 0.0008\, R_\sigma \quad \text{for} \quad R_\sigma > Ma$$
$$\Delta t^* < 0.0008\, Ma \quad \text{for} \quad R_\sigma < Ma.$$

If R_σ is greater than Ma the stability of the numerical scheme is governed by the vorticity equation while for R_σ less than Ma the stability of the numerical scheme is governed by the energy equation. Hence the stability criteria given above is different for R_σ greater than Ma and R_σ less than Ma. The stability criteria given above is for a square cavity. For a rectangular cavity with aspect ratio greater than one the stability criteria is somewhat more stringent (for an equal number of grid points in the X- and Y-directions). The new stability criteria are

$$\Delta t^* < 0.0008\, R_\sigma/A, \quad R_\sigma > Ma$$
$$\Delta t^* < 0.0008\, Ma/A, \quad R_\sigma < Ma.$$

To obtain a steady-state solution for a square cavity with $R_\sigma = 10{,}000$, $Pr = 1$ and a 41×41 grid it took 8 min of CPU time on DEC-10 computer.

RESULTS

A study of the pattern of streamlines and isotherms for various values of surface tension Reynolds number and Prandtl number should reveal the nature of thermocapillary flow during laser melting. We will confine our discussion primarily to the results obtained in the steady state. We will first consider the results obtained for the square cavity. In Fig. 2 we see the streamline pattern for surface tension Reynolds numbers of 400, 2000 and 10,000, respectively. When the surface tension Reynolds number is 400 one big cell fills the left half of the cavity. On account of the symmetry in the cavity it is sufficient to show one half of the cavity; in Figs. 2–8 the left half of the cavity is shown. When the surface tension Reynolds number reaches 2000 a small secondary cell begins to form at the bottom left corner of the cavity. When the surface tension Reynolds number is 10,000 the secondary cell becomes comparable to the primary cell at the top of the cavity. Although there is a dramatic change in the flow pattern as R_σ is increased from 400 to 10,000, there is no substantial change in the thickness of the surface layer. The surface layer is defined here as the layer near the interface which moves in the same direction as the fluid at the interface. In the present case, the fluid particle at the interface moves from the centre to the edge of the cavity. From Fig. 2 we infer that the thickness of the surface layer is almost constant as the surface tension Reynolds number increases from 400 to 10,000. This interesting feature of thermocapillary flow will be discussed in more detail a little later. In Fig. 3 the isotherm pattern is shown for a fluid with Prandtl number equal to 1 and for surface tension Reynolds numbers 400, 2000 and 10,000, respectively. When the surface tension Reynolds number is 400 the temperature profile in the cavity is governed by conduction and convection plays a minor role. As the

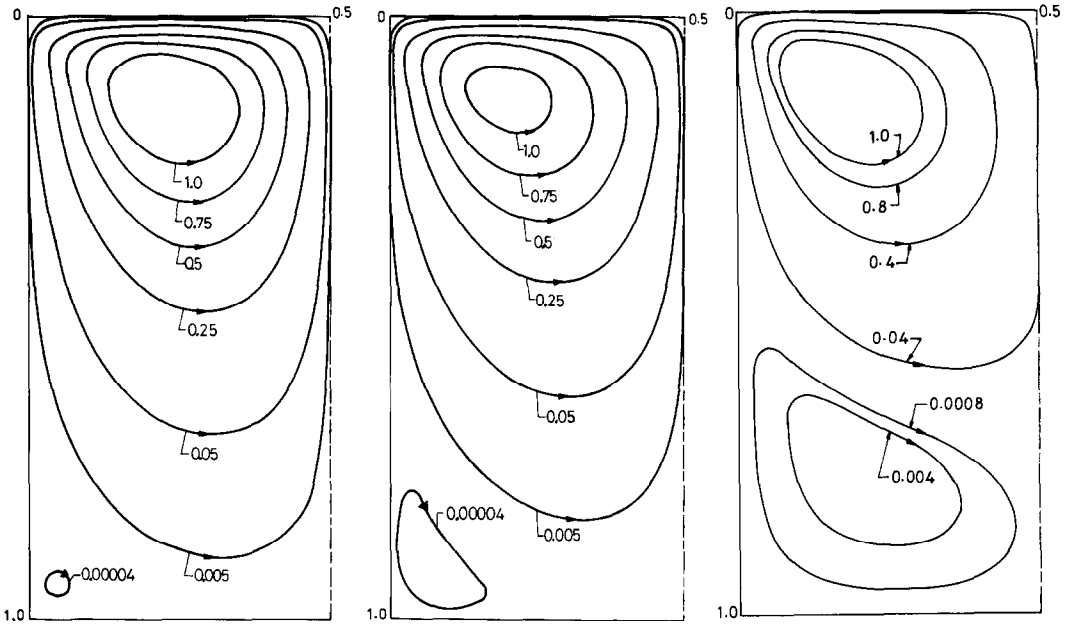

FIG. 2. Streamlines for a square cavity for various surface tension Reynolds numbers: (a) 400, (b) 2000, (c) 10,000.

surface tension Reynolds number increases to 2000 convection begins to show its presence by modifying the isotherms near the left wall of the cavity. At a Reynolds number of 10,000 convection influences the isotherms dramatically. The high velocity at the interface induces a large downward flow near the left wall of the cavity and hence the convection modifies the isotherms dramatically near the left wall of the cavity.

Figure 4 shows the isotherms for a fluid with a Prandtl number equal to 10 (typical of non-metals like silicon) and surface tension Reynolds numbers of 400, 2000 and 10,000 respectively. We find that convection begins to influence the isotherm pattern even when the surface tension Reynolds number is as low as 400. When the surface tension Reynolds number is 10,000 we find that most of the temperature variation occurs near the

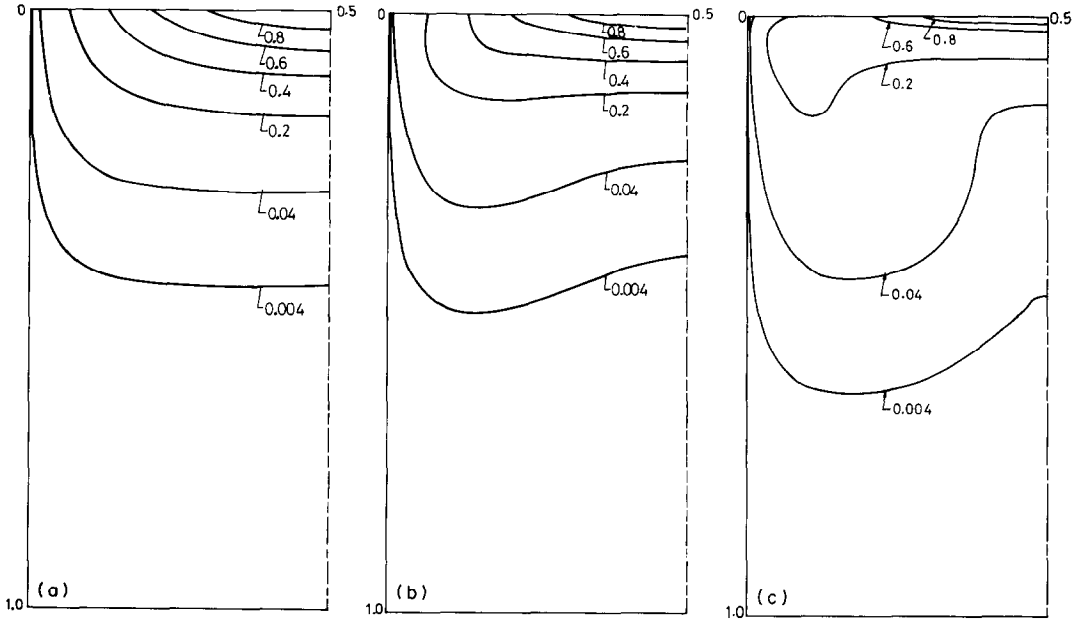

FIG. 3. Isotherms for a square cavity with $Pr = 1$, for various surface tension Reynolds numbers: (a) 400, (b) 2000, (c) 10,000.

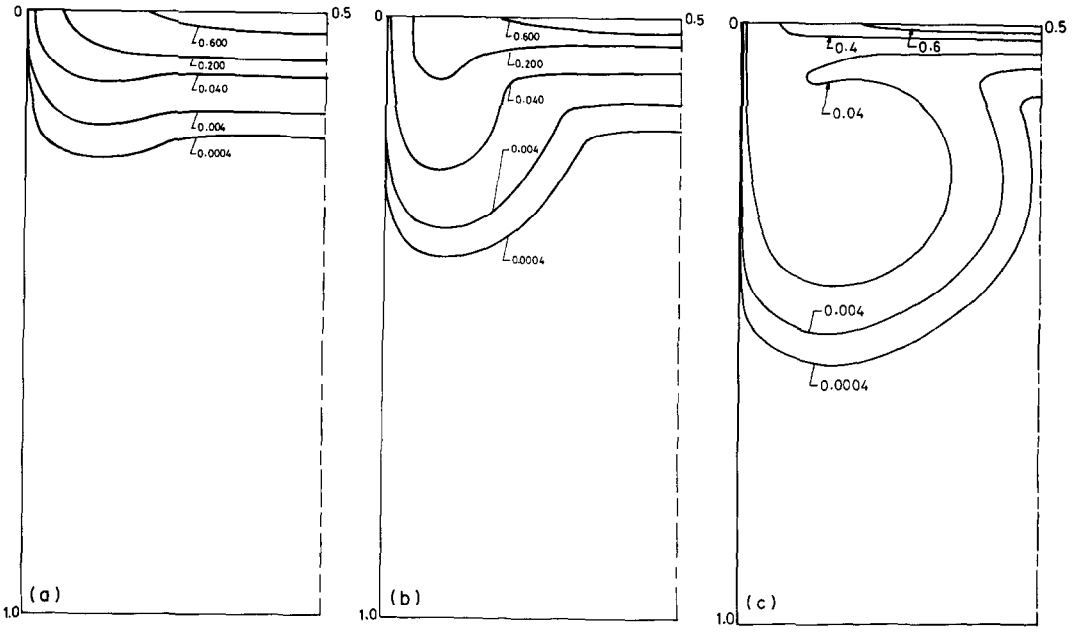

FIG. 4. Isotherms for a square cavity with $Pr = 10$ for various surface tension Reynolds numbers: (a) 400, (b) 2000, (c) 10,000.

interface within a thin thermal boundary layer. Figure 5 shows the isotherms for a fluid with Prandtl number equal to 0.1 (typical of molten metals like iron) and surface tension Reynolds number equal to 400, 2000 and 10,000, respectively. In this case we find that convection plays a relatively minor role and the isotherm pattern reflects the dominance of conduction. Although convection does not modify the shape of the isotherms, there is a discernable upward displacement of isotherms as the surface tension Reynolds number increases from 400 to 10,000. The role of convection is more clearly displayed in Fig. 6. Here we compare the isotherms obtained by neglecting convection (right panel) with that obtained by including convection (left panel) for a surface tension Reynolds number of 10,000 and a Prandtl number equal to 1. We observe that the

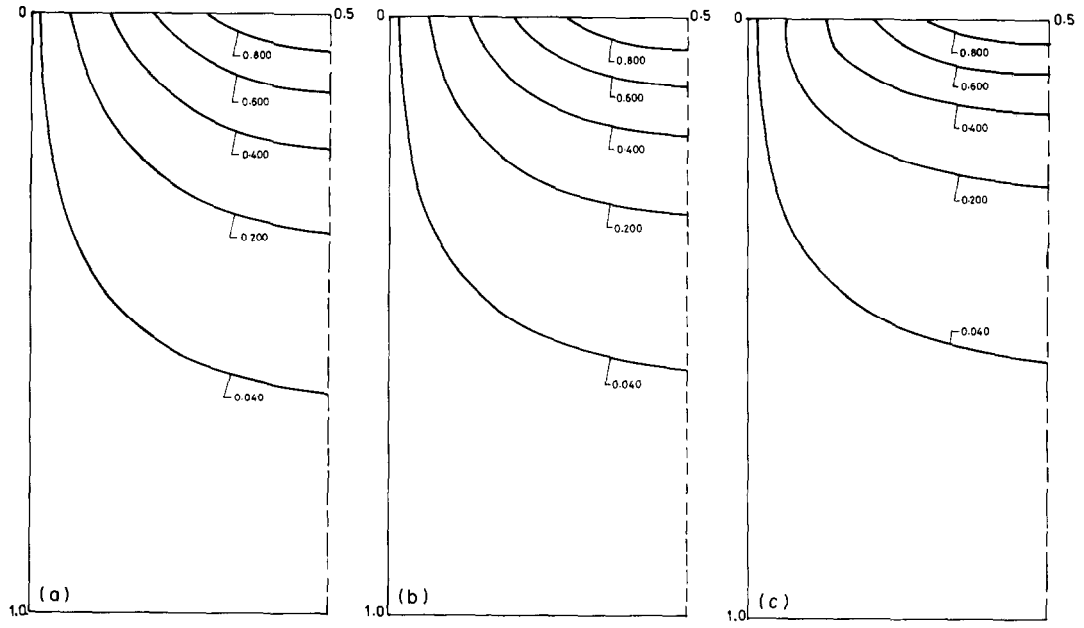

FIG. 5. Isotherms for a square cavity with $Pr = 0.1$ for various surface tension Reynolds numbers: (a) 400, (b) 2000, (c) 10,000.

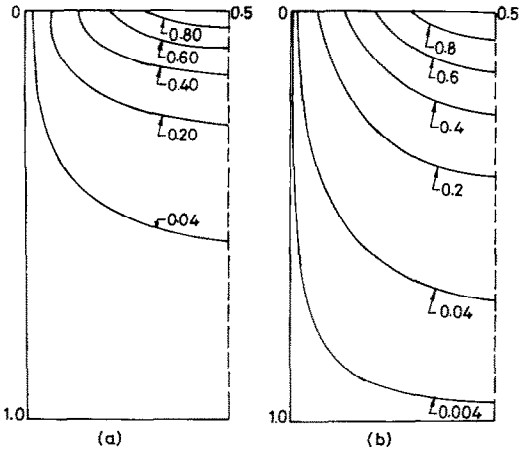

FIG. 6. Comparison of isotherm with convection for $R_\sigma = 10{,}000$ and $Pr = 0.1$ (a) and without convection (b).

isotherms are flatter when convection is included and the isotherms are displaced upwards. Hsu *et al.* [8] have presented a two-dimensional model for predicting the heat transfer and temperature profiles during laser melting and solidification. They assumed that the heat transfer in the melt was by conduction only. The present work shows clearly that we cannot neglect the role of convection while calculating the heat transfer and temperature profiles in the melt.

We have so far looked at the isotherms and streamlines for a square cavity for a range of surface tension Reynolds numbers and Prandtl numbers. In Fig. 7, the streamline and isotherm patterns are shown for a rectangular cavity with aspect ratio equal to 0.2. We observe once more that the surface layer is thin and in this case confined to the top third of the cavity. In Fig. 8 the streamline and isotherm pattern are shown for a rectangular cavity with aspect ratio equal to 5. In this case the surface layer is extremely thin and most of the deep cavity is a 'dead zone' with very slow moving fluid particles.

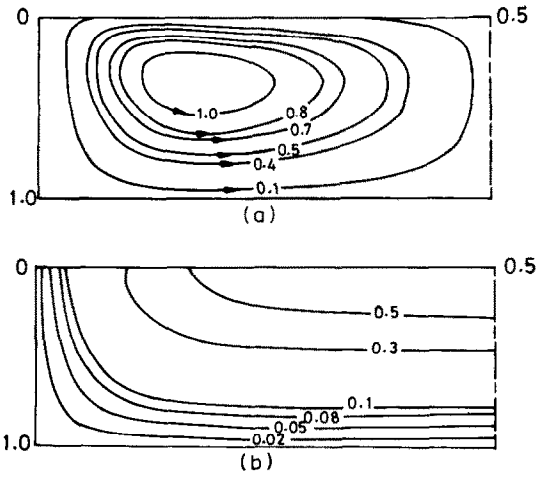

FIG. 7. Streamlines and isotherms for a rectangular cavity with aspect ratio equal to 0.2 with $R_\sigma = 2000$ and $Pr = 0.1$.

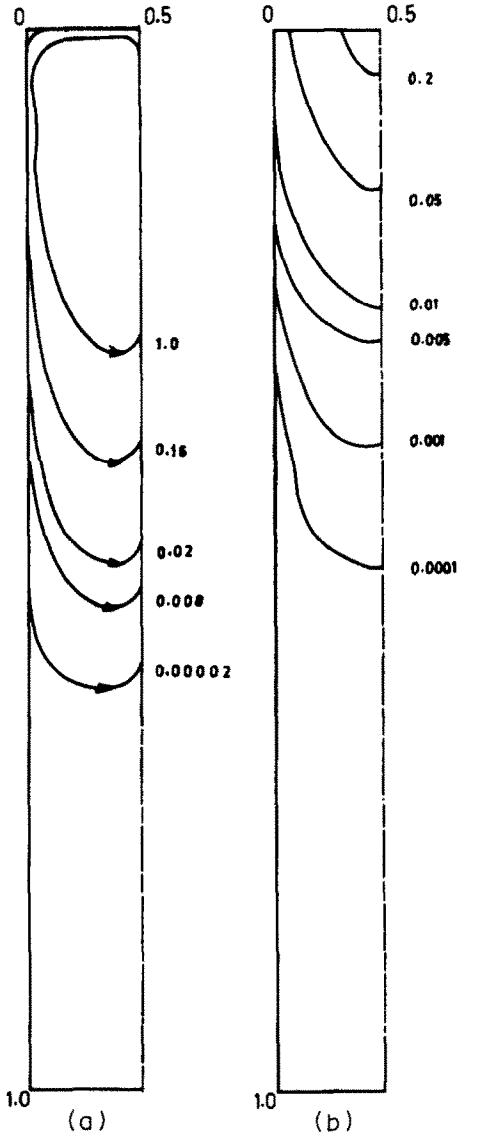

FIG. 8. Streamlines and isotherms for a rectangular cavity with aspect ratio equal to 5.0 with $R = 2000$ and $Pr = 0.1$.

In the present paper, we have assumed that the presence of laser results in a sinusoidal variation of temperature at the surface. The actual situation is much more complicated on account of the spatial variation of radiation across the laser beam and the spatial variation in the absorptivity of the surface of the molten material and the spatial variation in the heat loss from the surface. In Fig. 9 the spatial variation of non-dimensional heat flux along the surface is shown. We conclude that a sinusoidal variation of surface temperature implies a similar variation of heat flux when the surface tension Reynolds number is 100. At a surface tension Reynolds number of 1000, a sinusoidal variation of surface temperature implies a heat flux

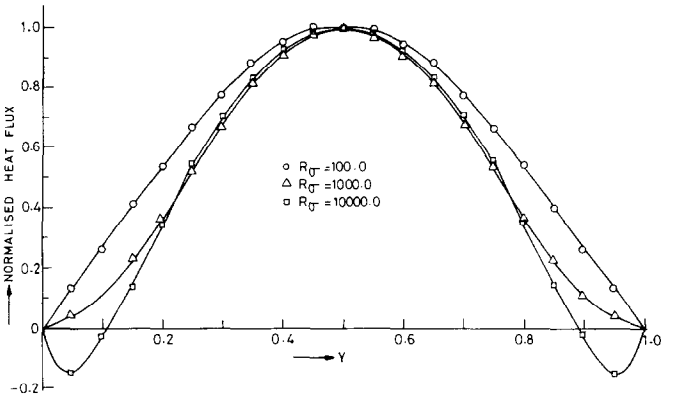

FIG. 9. Heat flux variation along the free surface.

variation which is more Gaussian-like. At a surface tension Reynolds number of 10,000, a sinusoidal variation of surface temperature implies regions of negative heat flux near the edge of the cavity. This is not unrealistic if the amount of laser energy absorbed near the edge of the cavity is less than the energy lost by convection and radiation. In Fig. 10 the variation of horizontal velocity (non-dimensionalised with respect to the horizontal velocity at the surface) with depth is shown for three different surface tension Reynolds numbers. We find that the shape of the horizontal velocity profile is very similar even though the surface tension Reynolds numbers range from 100 to 10,000. We discover also that the point at which velocity changes sign is almost the same. In other words the thickness of the surface layer is almost constant. This remarkable result could be useful for analysts who would like to obtain approximate analytical solutions for thermocapillary flow in a cavity. An approximate analytical solution will be very useful for reduction of computation time because 90% of the total CPU time (required to obtain the solution of Navier–Stokes equations and energy equation) is utilised for the solution of vorticity equation and streamfunction equation.

In Fig. 11 the variation of the maximum horizontal velocity in a square cavity is shown as a function of surface tension Reynolds number. In order to bring out the role of surface tension Reynolds number explicitly the non-dimensional horizontal velocity has been defined somewhat differently. We observe that at low surface tension Reynolds number the maximum horizontal velocity increases linearly with the surface tension Reynolds number while at high surface tension Reynolds number the maximum horizontal velocity

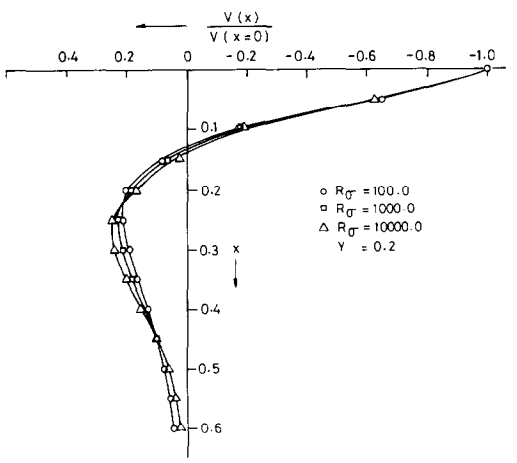

FIG. 10. Horizontal velocity profiles for various surface tension Reynolds numbers.

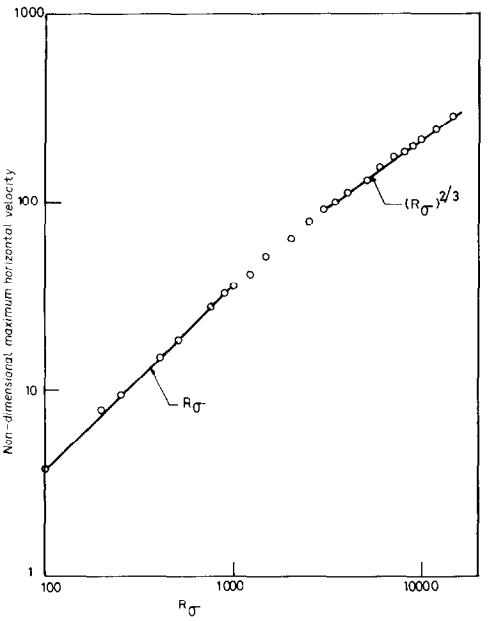

FIG. 11. Variation of non-dimensional maximum horizontal velocity profile as a function of surface tension Reynolds number.

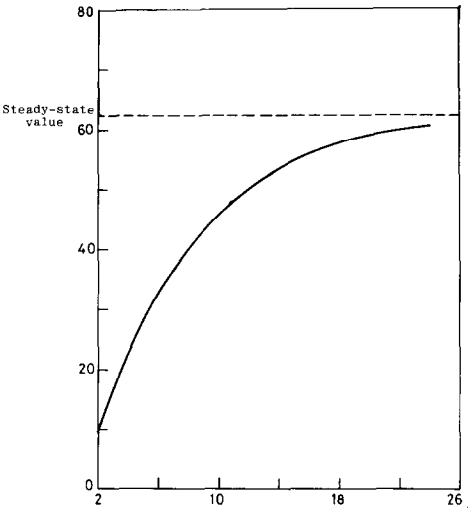

FIG. 12. Increase of non-dimensional maximum horizontal velocity with time.

varies as the surface tension Reynolds number to the power of two-thirds. Ostrach [8] had predicted this trend, by using dimensional analysis, for thermocapillary flow during crystal growth. In Fig. 12 the time taken for the thermocapillary flow in a square cavity to attain the steady state is shown. We can conclude from this figure that when the surface tension Reynolds number is 2000, the maximum horizontal velocity reaches 90% of its steady-state value when the non-dimensional time is 20. For laser melting of iron (with $W = L = 0.001$ m and $T_c - T_0 = 200$ K) this implies that steady state is reached in a time of 10 ms. If the laser scan speed is 1 cm s^{-1}, the fluid flow pattern attains a steady state while the laser moves by only 0.01 mm and hence a quasi-steady-state approximation may be appropriate.

CONCLUSIONS

The basic conservation equations of momentum and energy which govern the thermocapillary flow in a cavity during laser melting can be solved by standard finite-difference techniques. The results presented in this paper show that the inertia forces are dominant in the momentum equations and convective terms are important in the energy equation. The thickness of the surface layer is almost constant irrespective of the value of the surface tension Reynolds number. The temperature field is strongly influenced by convection if the surface tension Reynolds number is large or the fluid has high Prandtl number. The buoyancy driven flow is negligible compared to the thermocapillary flow in the conditions normally encountered in laser melting.

Acknowledgements—We thank Professor E. C. Subbarao, Director, Tata Research, Development and Design, Centre, Pune and Dr J. A. Sekhar, Defence Metallurgical Research Laboratory, Hyderabad, for several fruitful discussions. This work was supported by a project from Defence Research Development Organisation, Delhi.

REFERENCES

1. R. Mehrabian, S. Kou and A. Munitz, Laser surface melting and subsequent solidification. In *Laser–Solid Interactions and Laser Processing*. Materials Research Society, Boston (1978).
2. T. R. Anthony and H. E. Cline, Surface rippling induced by surface tension gradients during laser surface melting and alloying, *J. appl. Phys.* **48,** 3888–3894 (1977).
3. J. O. Wilkes and S. W. Churchill, The finite difference computation of natural convection in a rectangular cavity, *A.I.Ch.E. Jl* **12,** 161–166 (1966).
4. A. K. Sen and S. H. Davies, Steady thermocapillary convection in two dimensional slots, *J. Fluid Mech.* **121,** 163–186 (1982).
5. K. E. Torrance, Comparison of finite difference computations of natural convection, *J. Res. Natn. Bur. Stand.* **72B,** 281–301 (1968).
6. P. J. Roache, *Computational Fluid Dynamics* (revised edn). Hermosa, Albuquerque, NM (1976).
7. J. Szekely and M. R. Todd, Natural convection in a rectangular cavity: transient behaviour and two phase systems in laminar flow, *Int. J. Heat Mass Transfer* **14,** 467–482 (1971).
8. S. C. Hsu, S. Kou and R. Mehrabian, Rapid melting and solidification of a surface due to a stationary heat flux, *Met. Trans.* **11B,** 29–37 (1980).
9. S. Ostrach, Fluid mechanics in crystal growth, *J. Fluid Engng* **105,** 5–20 (1983).

UNE ETUDE NUMERIQUE DE L'ECOULEMENT THERMOCAPILLAIRE DANS UNE CAVITE RECTANGULAIRE PENDANT LA FUSION PAR LASER

Résumé—On étudie l'écoulement créé par le gradient de tension superficielle qui existe pendant une fusion laser. Les équations de Navier–Stokes et d'énergie exprimées à l'aide de fonction de courant-tourbillon sont résolues par la méthode "implicite à directions alternées". On montre que les forces d'inertie dans le bain influence fortement la configuration de l'écoulement dans le bain. La convection modifie les isothermes dans le bain pour un grand nombre de Reynolds de tension de surface et un grand nombre de Prandtl. L'écoulement sous l'effet de la pesanteur est trouvé négligeable en comparaison de celui relatif au gradient de tension superficielle dans la fusion par laser.

NUMERISCHE UNTERSUCHUNG DER OBERFLÄCHENSPANNUNGSGETRIEBENEN STRÖMUNG IN EINEM RECHTECKIGEN HOHLRAUM WÄHREND DES SCHMELZENS MIT LASER

Zusammenfassung—Die Strömung aufgrund des Gradienten der Oberflächenspannung, wie sie beim Schmelzen mit Laser entsteht, wurde numerisch untersucht. Die Navier–Stokes-Gleichungen und die Energiegleichung wurden in die Form von Wirbeltransport- und Stromfunktion gebracht und mit Hilfe der ADI-Methode gelöst. Es wird gezeigt, daß die Trägheitskräfte in der Schmelze das Strömungsbild stark beeinflussen. Die Konvektion in der Schmelze ändert die Isothermen bei hoher Oberflächenspannungs-Reynolds-Zahl und hoher Prandtl-Zahl. Die Strömung aufgrund von Auftriebskräften ist im Vergleich zur Strömung aufgrund des Gradienten der Oberflächenspannung vernachlässigbar.

ЧИСЛЕННОЕ ИССЛЕДОВАНИЕ ТЕРМОКАПИЛЛЯРНОГО ТЕЧЕНИЯ В ПРЯМОУГОЛЬНОЙ ПОЛОСТИ ПРИ ПЛАВЛЕНИИ ПОД ДЕЙСТВИЕМ ЛАЗЕРНОГО ИЗЛУЧЕНИЯ

Аннотация—Исследуется течение, вызванное градиентом поверхностного натяжения при плавлении под действием лазерного излучения. Неявным методом переменных направлений решены уравнения Навье–Стокса и энергии. Показано, что силы инерции в расплаве оказывают сильное влияние на режим течения. Конвекция в расплаве приводит к изменению изотерм при больших числах Рейнольдса для поверхностного натяжения и больших числах Прандтля. Показано, что течение, вызванное подъемной силой, пренебрежимо мало по сравнению с течением, вызванным градиентом поверхностного натяжения.